Science Advances

AAAS

advances.sciencemag.org/cgi/content/full/3/9/e1700841/DC1

Supplementary Materials for

Bication lead iodide 2D perovskite component to stabilize inorganic α-$CsPbI_3$ perovskite phase for high-efficiency solar cells

Taiyang Zhang, M. Ibrahim Dar, Ge Li, Feng Xu, Nanjie Guo, Michael Grätzel, Yixin Zhao

Published 29 September 2017, *Sci. Adv.* **3**, e1700841 (2017)
DOI: 10.1126/sciadv.1700841

This PDF file includes:

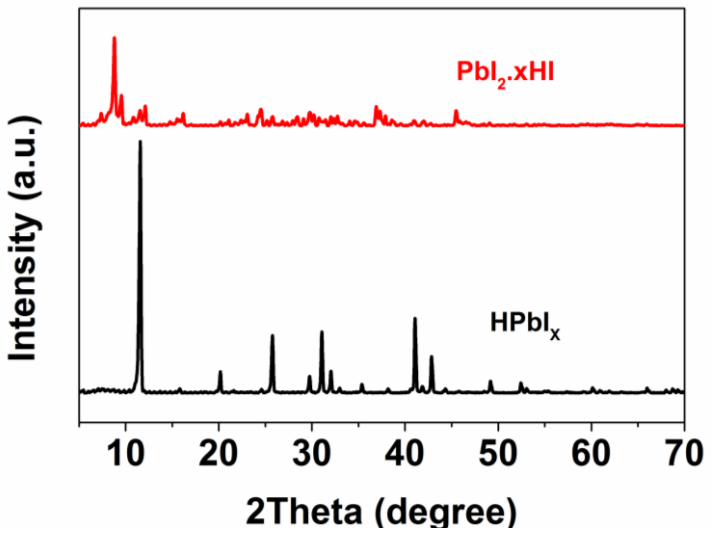

fig. S1. Comparative analysis of crystal structures of PbI_2•xHI and $HPbI_3$. XRD patterns of PbI_2·xHI and $HPbI_3$ powders.

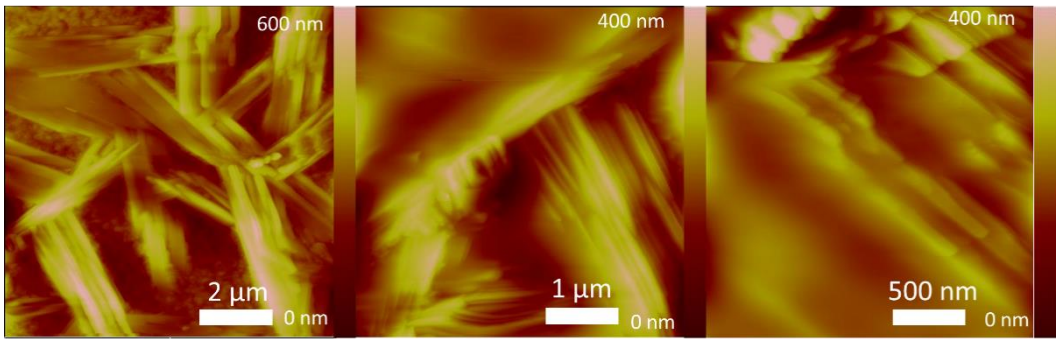

fig. S2. Morphology of $EDAPbI_4$ films. AFM images of $EDAPbI_4$ films.

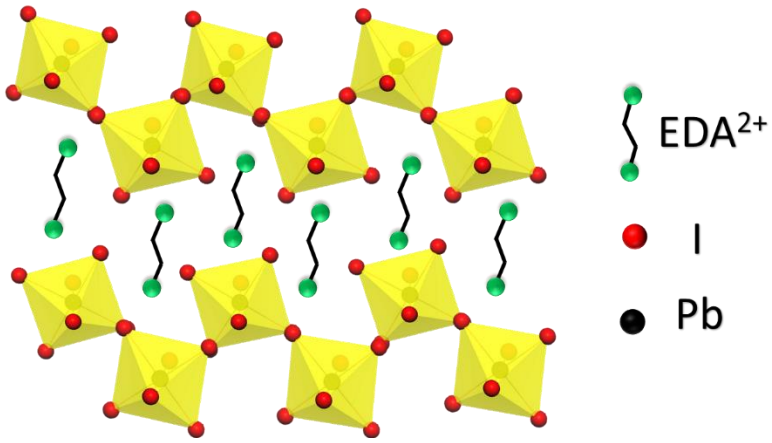

fig. S3. Schematic structure of (110) layered 2D films. Schematic structure of $EDAPbI_4$.

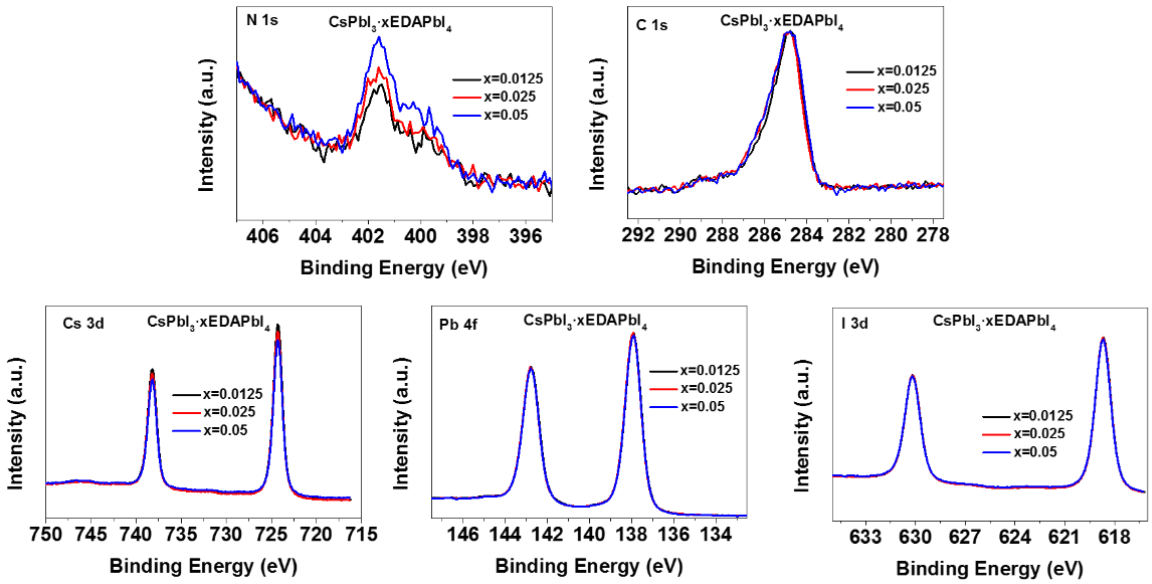

fig. S4. The organic compositions of $CsPbI_3$•x$EDAPbI_4$ films. XPS analysis of $CsPbI3{\cdot}xEDAPbI_4$ samples (x=0~0.05).

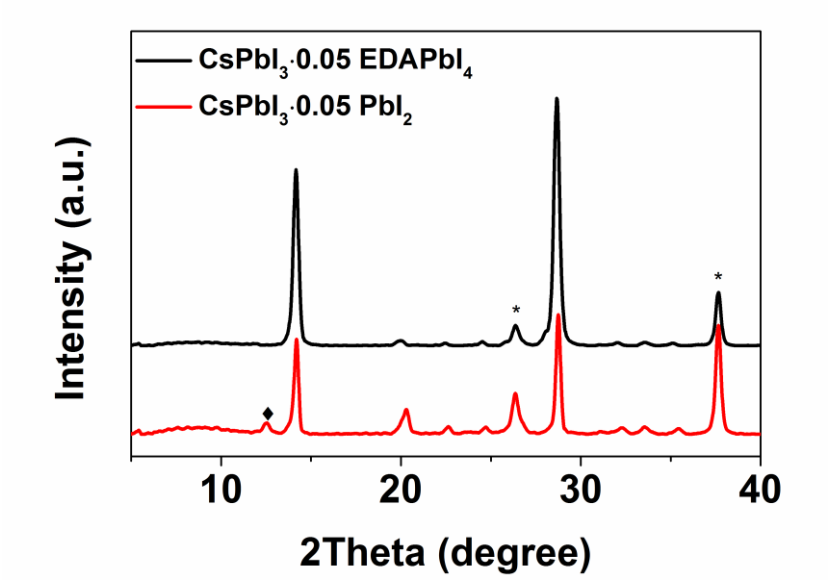

fig. S5. Characterization of $CsPbI_3$ + 0.05PbI_2 with or without $EDAI_2$. XRD pattern of $CsPbI_3$+0.05EDAPbI4 and $CsPbI_3$+0.05PbI_2 samples. The star is index to FTO pattern, the rectangle is index to PbI_2 peak.

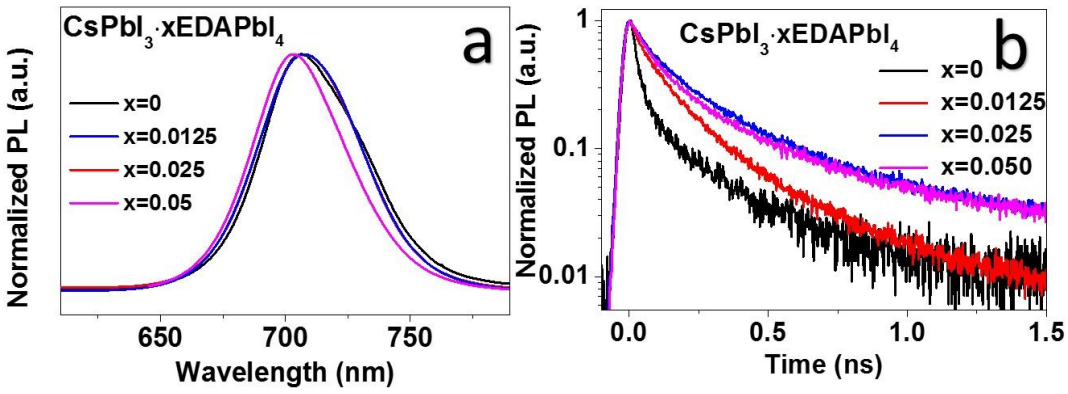

fig. S6. Effect of EDAPbI4 on the optical properties. (**a**) photoluminescence (**b**) time-resolved photoluminescence decay curves of $CsPbI_3{\cdot}x$EDAPbI$_4$ (x=0-0.05) perovskites.

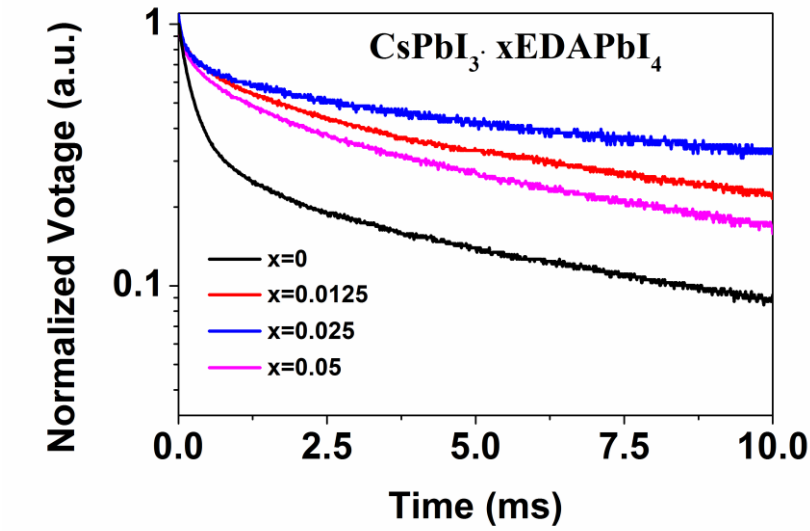

fig. S7. Effect of EDAPbI4 on the transient photovoltage behavior. Transient photovoltage decay curves of perovskite solar cells based on $CsPbI_3{\cdot}x$EDAPbI$_4$ samples (x: 0–0.05).

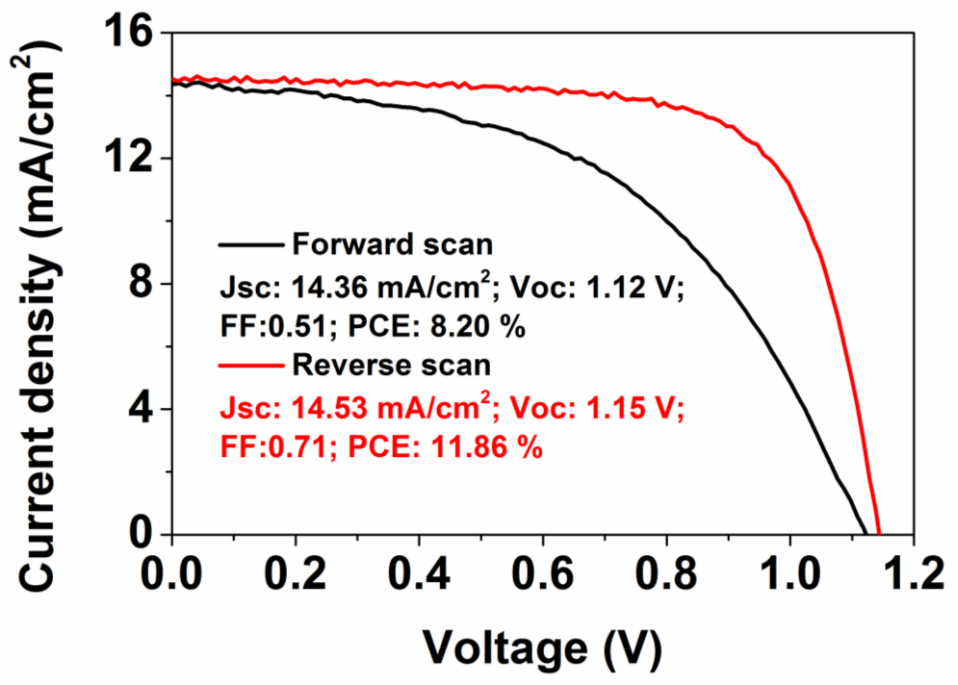

fig. S8. Hysteresis behavior of $CsPbI_3$•0.025$EDAPbI_4$-based device. A typical forward and reverse scan J-V curve of the perovskite solar cells based on $CsPbI_3$·0.025$EDAPbI_4$ samples.

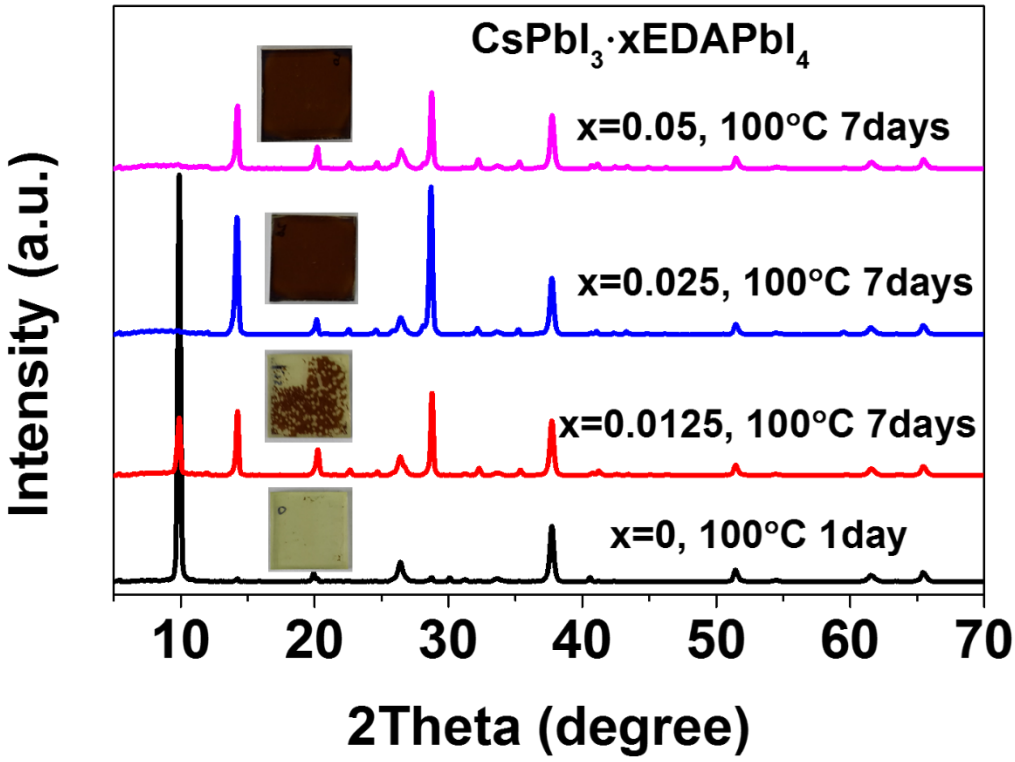

fig. S9. Effect of $EDAPbI_4$ on the phase stability of $CsPbI_3$•x$EDAPbI_4$ perovskite films. XRD patterns of $CsPbI_3$·x$EDAPbI_4$ film heated at 100 °C for 7days (1 day for x=0 samples).

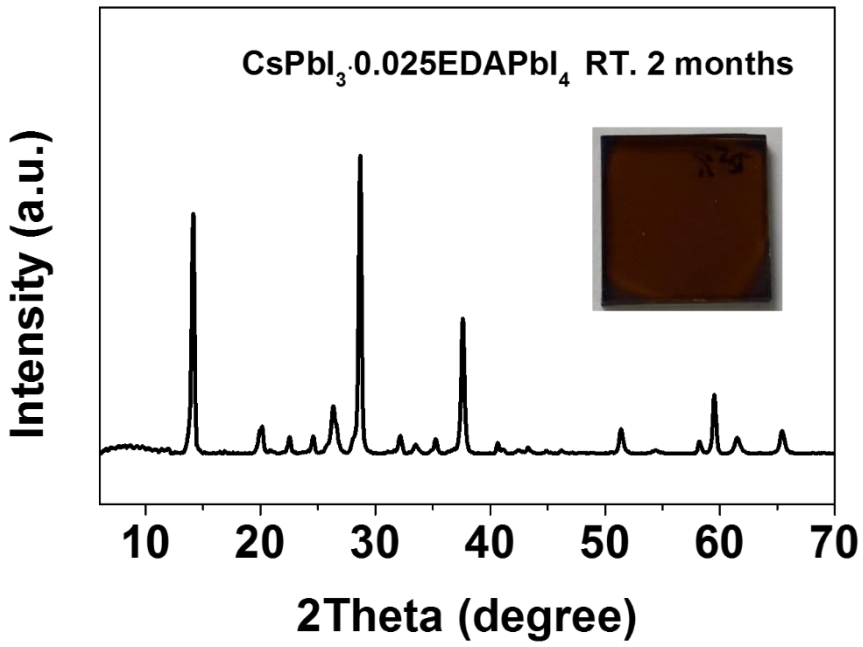

fig. S10. Phase stability of CsPbI3•0.025EDAPbI4 perovskite film under room temperature. XRD patterns of CsPbI3·0.025EDAPbI4 film after aged at room temperature in a drybox for two months.

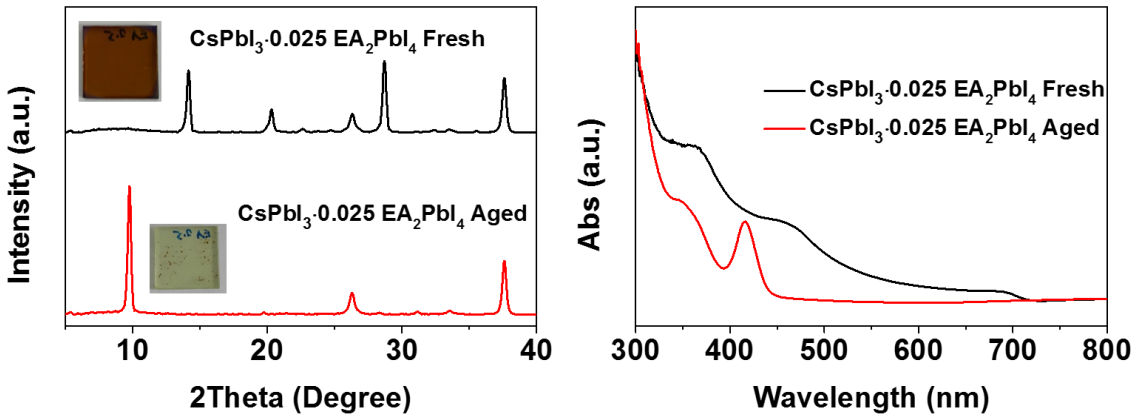

fig. S11. Phase stability of CsPbI3•0.025EA2PbI4-based films. XRD pattern and UV-vis spectra of $CsPbI_3 \cdot 0.05EA_2PbI_4$ films freshly prepared and aged for 1 day at room temperature.

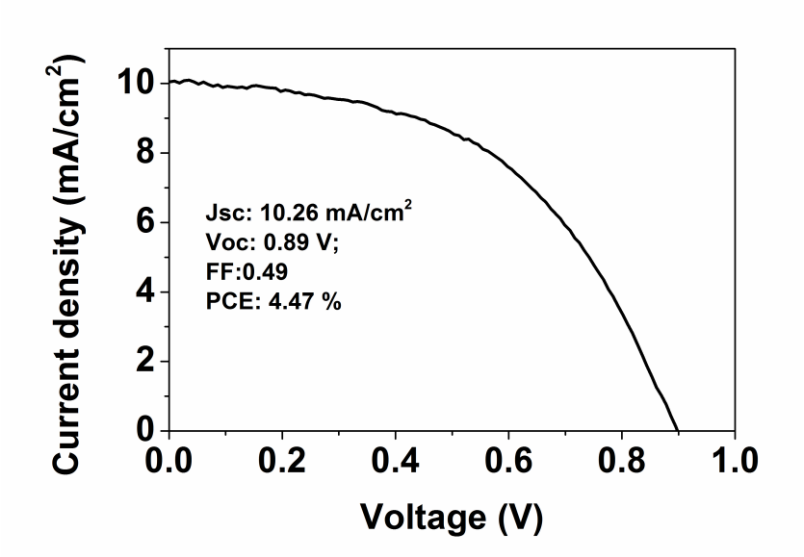

fig. S12. Device performance of $CsPbI_3$•0.025EA_2PbI_4-based solar cell. Champion J-V curves of $CsPbI_3$·0.025EA_2PbI_4 perovskite based solar cells.

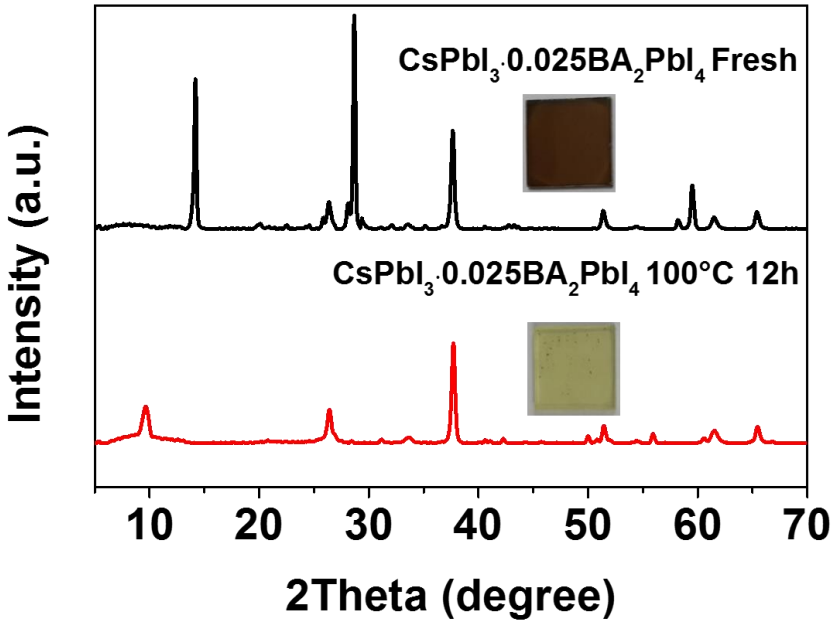

fig. S13. Phase stability of $CsPbI_3$•0.025BA_2PbI_4-based films. XRD patterns of $CsPbI_3$·0.025BA_2PbI_4 films freshly prepared and aged for 12 hrs at 100°C.

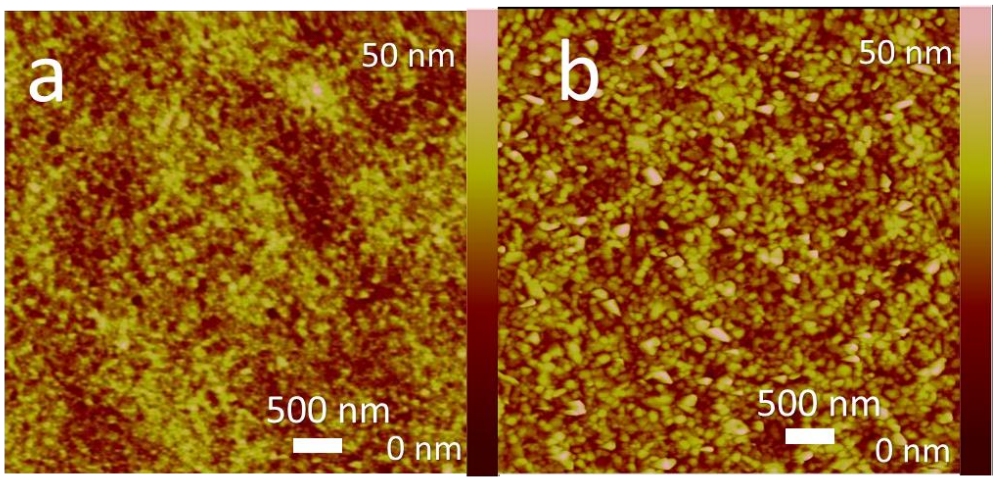

fig. S14. Effect of $CsPbI_3$•0.025BDAPbI4 and $CsPbI_3$•0.025EDBEPbI4 2D perovskite component on the evolution of morphology. AFM images of $CsPbI_3$·0.025BDAPbI4 (**a**) and $CsPbI_3$·0.025EDBEPbI4 (**b**).

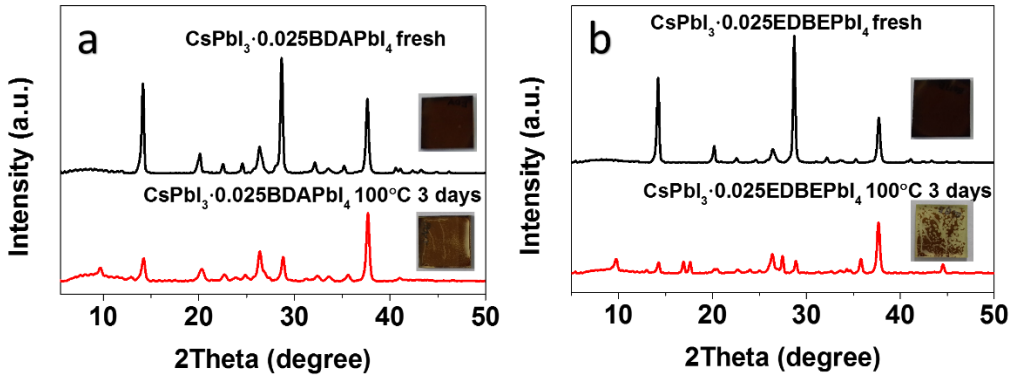

fig. S15. Phase stability of $CsPbI_3$•0.025BDAPbI4 and $CsPbI_3$•0.025EDBEPbI4 films. XRD patterns of $CsPbI_3$·0.025BDAPbI4 (**a**) and $CsPbI_3$·0.025EDBEPbI4 (**b**) films freshly prepared and aged for 3days at 100°C.